

# A stable Algebraic Spin Liquid in a Hubbard model

S. R. Hassan,<sup>1</sup> P.V. Sriluckshmy,<sup>1</sup> Sandeep K Goyal,<sup>1,2</sup> R. Shankar,<sup>1</sup> and David Sénéchal<sup>3</sup>

<sup>1</sup>*The Institute of Mathematical Sciences, C.I.T. Campus, Chennai 600 113, India*

<sup>2</sup>*School of Chemistry and Physics, University of KwaZulu-Natal, Durban, South Africa*

<sup>3</sup>*Département de physique and RQMP, Université de Sherbrooke, Sherbrooke, Québec, Canada J1K 2R1*  
(Dated: August 28, 2012)

We show the existence of a stable Algebraic Spin Liquid (ASL) phase in a Hubbard model defined on a honeycomb lattice with spin-dependent hopping that breaks time-reversal symmetry. The effective spin model is the Kitaev model for large on-site repulsion. The gaplessness of the emergent Majorana fermions is protected by the time reversal (TR) invariance of this model. We prove that the effective spin model is TR invariant in the entire Mott phase thus ensuring the stability of the ASL. The model can be physically realized in cold atom systems and we propose experimental signals of the ASL.

The concept of a spin liquid as a Mott phase without any local order was put forward by Anderson [1]. Its relevance to the physics of high temperature superconductors[2, 3] led to the development of a gauge theory of spin liquids [3, 4], analogous to quantum electrodynamics(QED). The spinons are the counterpart of electrons in QED and the visons, another emergent excitation, are the counterpart of the photon. Attempts at understanding the emergence of fermionic quasi-particles in spin systems in analogy with the anyonic quasi-particles in fractional quantum Hall systems has led to a general theory of quantum/topological order in spin liquids[5]. Experimental evidence for a spin liquid ground state has been seen, for instance, in the organic material  $\kappa$ -(BEDT-TTF)<sub>2</sub>Cu<sub>2</sub>(CN)<sub>3</sub>[6].

Frustration in magnetic interactions and quantum fluctuations tend to prevent magnetic ordering. Thus ASLs have primarily been studied in frustrated spin-1/2 Heisenberg anti-ferromagnets.[7–9]. The ASL shows power law decay not only for spin correlations but many other local order parameters as well. Hence it is intrinsically susceptible to one of them ordering and inducing a spinon gap. Thus any realization of this phase must be accompanied by a mechanism of ensuring its stability.

Kitaev[10] constructed an exactly solvable anisotropic spin-1/2 model on a honeycomb lattice that exhibits the important properties of an ASL. It can be expressed as a model of two gapless Majorana-Dirac fermions (spinons) interacting with  $Z_2$  gauge fields (visons). A remarkable feature of the model is that the magnetic flux associated with every plaquette is conserved, as a result of which the visons are static. Consequently, while multi-spin operators that conserve flux have algebraic correlations, those which do not, including the single spin operators, are extremely short ranged[11]. However, it has been shown that, for a certain class of perturbations that break these conservation laws, the spin-spin correlations become algebraic as well[8, 9]. ASLs are thus realized in such perturbed models. The stability of the ASL in the Kitaev model is due to time reversal (TR) symmetry: the two Majorana-Dirac fermions combine to form a *single* Dirac

fermion, with an energy spectrum that cannot have a gap without breaking TR symmetry. An exactly solvable spin-3/2 model with algebraic spin correlations has also been constructed [14].

The ASL has not yet been realized in a model of interacting fermions, though attempts have been made speculating the possible means of doing so[15–17]. However, it was shown[18] that a short-ranged spin liquid (SRSL) emerges between the semi-metal and the Néel phases in a Hubbard model defined on a honeycomb lattice. A recent work claims otherwise[19].

The above discussion suggests that a Hubbard model, which is described effectively by the Kitaev honeycomb spin model in the large  $U$  limit, is a good candidate for realizing an ASL. Such a model was proposed by Duan *et al.* as a way of realizing the Kitaev model[10] in cold atom systems[20]. This model, which we henceforth call the Kitaev-Hubbard model, has anisotropic spin-dependent hopping which leads to the high degree of frustration in the effective spin model. The Hamiltonian of this model is

$$H = \sum_{\langle ij \rangle_\alpha} \left\{ c_i^\dagger \left( \frac{t + t' \sigma_\alpha}{2} \right) c_j + \text{H.c} \right\} + U \sum_i n_{i\uparrow} n_{i\downarrow} \quad (\text{S1})$$

where  $c_{i\sigma}$  annihilates a fermion of spin projection  $\sigma = \uparrow, \downarrow$  at site  $i$  (the spin index is implicit in the first term),  $\sigma_\alpha$  ( $\alpha = x, y, z$ ) are the Pauli matrices,  $n_\sigma \equiv c_\sigma^\dagger c_\sigma$  is the number of fermions of spin  $\sigma$  at site  $i$ , and  $\langle ij \rangle_\alpha$  denotes the nearest-neighbor pairs in the three hopping directions of the lattice (see Fig. S1).

At  $t' = 0$ , the model reduces to the simple spin- and TR-invariant, nearest-neighbor Hubbard model[18, 19]. The term proportional to  $t'$  is a spin-dependent hopping term and breaks TR symmetry,  $SU(2)$  spin symmetry and the three-fold spatial rotation symmetry of the  $t' = 0$  model. It is however invariant under a spatial rotation of  $2\pi/3$  combined with a spin rotation of  $2\pi/3$  about the (111) spin axis. At  $t' = t$ , the one-body part of the Hamiltonian is a combination of the projection operators  $\frac{1}{2}(1 + \sigma_\alpha)$ . Thus, only those electrons that are

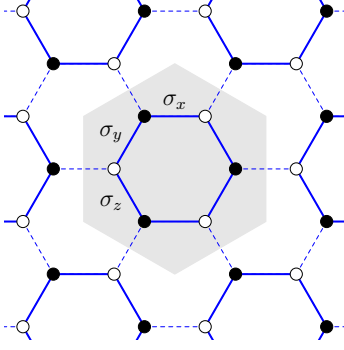


FIG. S1: (color online) The honeycomb lattice with the two sublattices marked by white and black dots. The six-site cluster used in this work is shown as the shaded area. The  $\sigma_i$  label the different spin-dependent hopping directions (blue solid lines), whereas the inter-cluster bonds are shown as dashed lines.

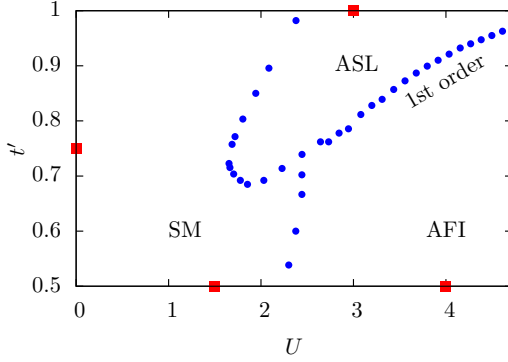


FIG. S2: (color online) The phase diagram of the Kitaev-Hubbard model at half-filling, showing the phases. The transition from the AFI to the ASL phase is discontinuous. The red squares correspond to the parameter values at which the spectral graphs have been plotted in Fig. S3.

spin-polarized in the  $\alpha^{\text{th}}$  direction can hop along the  $\alpha$  bonds. At this value of  $t'$ , the effective low-energy spin model, at half-filling and large  $U$ , is the Kitaev honeycomb model.[20, 21]

At  $U = 0$  and  $t' = 1$  the single particle spectrum of this model shows four distinct bands, each of which has a non zero Chern number  $\nu$ [22]. The top and the bottom bands have  $\nu = 1$ , while the two middle bands, with  $\nu = -1$ , are connected at the Dirac points. At  $t' = 1$ , the top two as well as the bottom two bands are gapped. As  $t'$  is decreased, this gap shrinks and finally closes at  $t' = 0.717$ . The existence and locations of Dirac points can be experimentally measured in optical lattice systems[23].

As mentioned earlier, at  $t' = t$ ,  $U \rightarrow \infty$ , the model is analytically tractable and as we show later, is an ASL. We have computed the extent of the ASL phase using Cluster Perturbation Theory[1] (CPT) and the Variational Cluster Approximation (VCA).[4] These numerical techniques allow us to map the charge-gap of the model on to

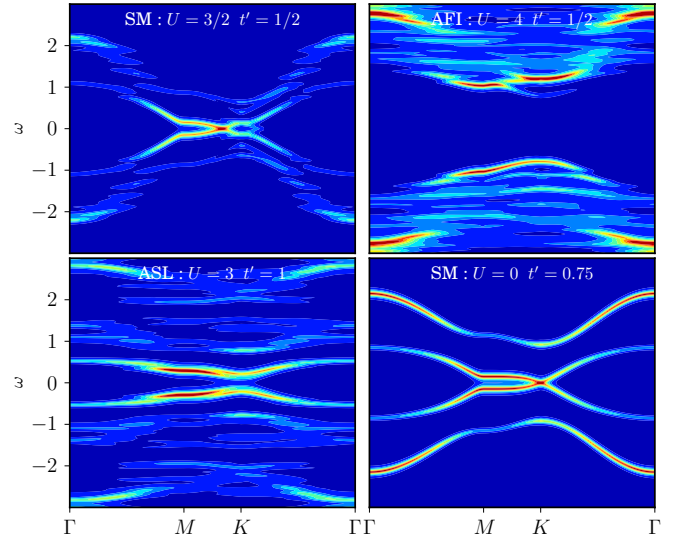


FIG. S3: Spectral functions of the Kitaev-Hubbard model, computed using CPT, as a function of energy ( $\omega$ , y-axis) and momentum ( $k$ , x-axis) for the four sets of parameter values marked by the squares in Fig. S2, red indicating maximum value and blue indicating minimum values. The spectrum is gapless only for the SM.  $\Gamma$ ,  $M$  and  $K$  represent the high symmetry points of the Brillouin zone.

the  $t' - U$  plane, and to calculate the extent of the Néel phase. VCA also allows us to find out whether or not the transitions out of the Néel phase are continuous. However, the same cannot be done for the Mott transitions to the spin-liquid phases for which a cluster dynamical mean field technique would be required.

Setting  $t = 1$ , we study the phase diagram of the Kitaev-Hubbard model from  $t' = 1$  to  $t' = 0.5$ . Our results are summarized in Fig. S2. At low  $U$  there is a TR-breaking semi-metallic phase (SM), characterized by charged, spin-1/2 fermionic quasi-particles. This phase exists in the region  $1 > t' > 0.5$  and  $U \lesssim 2.4$ . When  $U \approx 2.4$  and  $t' = 1$ , there is a Mott transition from the SM to the ASL phase, which then extends for large values of  $U$  at this  $t'$ . Between  $U \gtrsim 1.5$  and  $U \lesssim 2.4$  and with steadily decreasing  $t'$ , the system starts off in the SM phase, then makes a transition into the ASL phase and finally re-enters the SM phase, wherein it continues to live till  $t' = 0.5$ . At values of  $U$  greater than 2.4, decreasing  $t'$  destabilizes the ASL phase and brings about a transition to the anti-ferromagnetic (Néel) (AFI) phase. The width of the ASL phase in the  $t'$  variable is maximum at  $U \approx 2.4$ , extending from  $t' = 1$  to  $t' \approx 0.7$ .

The ASL phase is bounded by the AFI and SM phases and is hence not connected with the possible short-ranged spin liquid at  $t' = 0$ [18, 19]. The SM and AFI phases do not have quasi-particles with fractional quantum numbers or statistics. Thus the ASL is topologically distinct from the SM and the AFI and we expect the transitions between them to be discontinuous.

Using CPT, we obtain spectral functions corresponding to each of the three phases and plot them in Fig. S3. Our numerical computations show that the transition between the AFI and ASL phases is discontinuous (first-order) as expected. It is intriguing that the single particle bands of opposite Chern numbers remain gapped in the same range of values of  $t'$  as the existence of the ASL. This seems to indicate that geometric phase effects may play an important role in this model.

We study the ASL spin-spin correlations by deriving an effective, large- $U$  spin Hamiltonian of the Kitaev-Hubbard model at half filling. To leading order in  $1/U$ , this effective Hamiltonian is

$$H^{(2)} = \sum_{\langle ij \rangle_\alpha} \left[ \frac{(1-t'^2)}{U} \mathbf{S}_i \cdot \mathbf{S}_j + \frac{2t'^2}{U} S_i^\alpha S_j^\alpha \right] \quad (\text{S2})$$

This is a combination of the Heisenberg and Kitaev models. The effective Hamiltonian (S2) is TR symmetric, and this is thus responsible for the gaplessness of the Majorana spinons. Using charge-conjugation symmetry, we have analytically proved that the effective spin model is TR symmetric to all orders in  $1/U$  (see Supplementary Information). Therefore, the spinons remain gapless in the Mott phase. As mentioned earlier, in the Kitaev model, conservation laws cut off the spin-spin correlations beyond nearest neighbors[11]. Therefore, in order to analyze these correlations, we need to consider higher order terms.

We have calculated the next order term in the effective spin Hamiltonian and obtained

$$\begin{aligned} H^{(4)} = & \sum_{\substack{\langle ij \rangle_\alpha \\ \beta \neq \alpha}} \left[ \frac{(t'^4 - 1)}{U^3} \mathbf{S}_i \cdot \mathbf{S}_j - \frac{2t'^4}{U^3} S_i^\alpha S_j^\alpha \right. \\ & \left. - \frac{2t'^2}{U^3} (S_i^\alpha S_j^\beta + S_j^\alpha S_i^\beta) \right] + \sum_{\langle \langle ij \rangle \rangle_{\alpha\beta}} \left[ \frac{(1-t'^2)^2}{4U^3} \mathbf{S}_i \cdot \mathbf{S}_j \right. \\ & \left. + \frac{t'^2 - t'^4}{2U^3} (S_i^\alpha S_j^\alpha + S_i^\beta S_j^\beta) + 3 \frac{t'^2}{U^3} S_i^\alpha S_j^\beta \right] \quad (\text{S3}) \end{aligned}$$

where  $\langle ij \rangle_\alpha$  denote nearest neighbors in the  $\alpha$  direction and  $\langle \langle ij \rangle \rangle_{\alpha\beta}$  denote next-nearest neighbors reached by first moving in the  $\alpha$  direction and then in the  $\beta$  direction.

The spin-spin correlation is,

$$g(\mathbf{r}, t) = \left\langle T \left( S_{\mathbf{r}l}^\alpha(t) S_{\mathbf{0}l}^\beta(0) \right) \right\rangle \quad (\text{S4})$$

where  $\mathbf{r}$  is a site of the Bravais lattice,  $l$  is the sublattice index. We compute this perturbatively in the fermionic representation of the spins,[7] in which the Majorana fermion operators  $c_i$  and  $b_i^\alpha$  are defined as follows:

$$\begin{aligned} \sigma_i^\alpha &= ic_i b_i^\alpha, & \{c_i, c_j\} &= 2\delta_{ij} \\ \{b_i^\alpha, b_j^\beta\} &= 2\delta_{\alpha\beta} \delta_{ij}, & \{c_i, b_j^\alpha\} &= 0 \end{aligned} \quad (\text{S5})$$

The physical subspace is defined by the constraint

$$c_i b_i^x b_i^y b_i^z |\psi\rangle_{\text{phys}} = |\psi\rangle_{\text{phys}} \quad (\text{S6})$$

In terms of these Majorana fermions, the leading order Hamiltonian is,

$$\mathcal{H}_0 = J \sum_{\langle ij \rangle_\alpha} ic_i c_j ib_i^\alpha b_j^\alpha \quad (\text{S7})$$

where  $J = \left( \frac{1+t'^2}{U} - \frac{1+t'^4}{U^3} \right)$ . This Hamiltonian describes Majorana fermions ( $c_i$ ), which we refer to as spinons, propagating in the background of static  $Z_2$  gauge fields ( $u_{\langle ij \rangle_\alpha} = ib_i^\alpha b_j^\alpha$ ). The spin-spin correlation functions therefore factorize into propagators of the  $c_i$  operators. Since the spin operators create two units of flux on adjoining plaquettes, the Majorana fermion propagators are in the background of an even number of fluxes at a few points.

We are interested in the asymptotic form of the leading order correction,  $g^{(2)}(\mathbf{r}, t)$ , when  $|\mathbf{r}|, t \rightarrow \infty$ . Tikhonov *et al.* [9] have shown that in this limit, the propagators are the same as those in the flux-free background. Their result can be physically understood by noting that the particles hopping far way from the flux pairs will not pick up any phases from them. Thus we can expect the long wavelength modes to be insensitive to a few localized flux pairs.

To compute the asymptotic form or the propagators, we can derive the continuum theory of the low-energy modes in the flux-free background. The Hamiltonian (S47), when  $ib_i^\alpha b_j^\alpha = 1$ , reduces to nearest-neighbor hopping on a honeycomb lattice just as in graphene. Graphene has low-energy Dirac quasi-particles about two points,  $\mathbf{K}$  and  $\mathbf{K}'$ , in the Brillouin zone. However, since the  $c$  fermions are Majorana fermions, the excitations exist only over half the Brillouin zone. Thus the low-energy modes constitute a single Dirac quasi-particle. The continuum theory is derived by introducing slowly varying fields  $\psi_l(\mathbf{r})$  such that

$$c_{\mathbf{r}l}(t) = \frac{1}{2} \left( e^{i\mathbf{K} \cdot \mathbf{r}} \psi_l(\mathbf{r}, t) + e^{-i\mathbf{K} \cdot \mathbf{r}} \psi_l^\dagger(\mathbf{r}, t) \right) \quad (\text{S8})$$

$\psi(\mathbf{r}, t)$  satisfies the gapless Dirac equation. Any mass term for a *single* fermion breaks TR invariance. Thus the gaplessness is protected by the TR invariance of the effective spin model.

We have calculated the dynamical spin-spin correlations in the long-wavelength limit following the methods of Tikhonov *et al.*, [9] (see Supplementary Information):

$$\begin{aligned} \langle S_{\mathbf{r}l}^z(t) S_{\mathbf{0}l}^z(0) \rangle &= (-0.56 \cos(2\mathbf{K} \cdot \mathbf{r}) \gamma_1^2 + 1.13 \gamma_1 \gamma_2 + 0.88 \gamma_2^2) \det G \\ &+ 0.28 \gamma_1^2 \text{tr}(\tau_x G \tau_x G) + (0.56 \gamma_1^2 + 0.16 \gamma_1 \gamma_2) \text{tr}(G \tau_x G) \\ &+ (0.28 \gamma_1^2 + 0.02 \gamma_2^2 + 0.16 \gamma_1 \gamma_2) (\text{tr} G)^2 \end{aligned} \quad (\text{S9})$$

where  $\gamma_1 = -\frac{2t'^2}{U^3}$ ,  $\gamma_2 = \frac{3t'^2}{2U^3}$  and  $\mathbf{K}$  is the Dirac point  $(2\pi/3, 2\pi/3\sqrt{3})$  and

$$G = (\boldsymbol{\tau} \cdot \mathbf{r} - Jt\mathbb{I}) \frac{1}{4\pi} \frac{1}{(\mathbf{r}^2 - J^2t^2)^{\frac{3}{2}}}. \quad (\text{S10})$$

Here  $t$  is the time,  $\boldsymbol{\tau} = (\tau^x, \tau^y)$  are the Pauli spin matrices.

Using equation (S51) and (S10), we find that the long-wavelength correlation function falls off as  $1/r^4$ . This algebraic decay has also been seen for single-spin perturbations studied in Ref. 9. Although the prefactor is extremely small ( $\sim 1/U^6$ ), this is the leading behavior at long distances. Therefore the effect of the perturbation cannot be neglected for any value of  $U$ , however large. Indeed, we can expect the strength of these correlations to grow as  $U$  decreases. This proves the existence of the ASL in the Kitaev-Hubbard model.

Thus, at large  $U$ , the leading order contribution to the spin susceptibility is independent of  $U$  as in the Kitaev model, whereas the next order contribution goes as  $(t/U)^6$ . The  $U$  dependence of the spin susceptibility will hence be of the form  $\chi = a + b(t/U)^6$ , where  $a$  and  $b$  are constants independent of  $U$ . Experimental methods for measuring the spin susceptibility in cold atom systems have recently been developed.[27] Thus susceptibility measurements as a function of  $U$  can provide evidence for the existence of the ASL in this model.

The stability of the ASL in this model comes from the preservation of TR symmetry. We have investigated the possibility of spontaneous breaking of TR symmetry and the consequent emergence of a chiral spin liquid (CSL) with a spinon gap (see Supplementary Information). In the fermionized version[10] of the effective spin model, where  $H_{\text{eff}} = H^{(2)} + H^{(4)}$ , we use a mean-field theory in which the vison and the spinon sectors are decoupled. This mean-field theory is exact for the Kitaev model, which is obtained by putting  $t' = 1$  in  $H^{(2)}$ . We find that the CSL solutions occur only for  $U \lesssim 1.6$  and for  $0.5 \leq t' \leq 1$ , and thus are not seen in the Mott regime  $U \gtrsim 2.4$ . In Fig. S7, we plot the spinon gap as a function of  $U$  for  $t' = 1$ .

In conclusion, we have shown that the Kitaev-Hubbard model, shows a Mott transition from a semi-metallic phase, to an algebraic spin-liquid phase. The former breaks time-reversal symmetry whereas the latter preserves it. The ASL is stabilized by TR symmetry. We have proved the TR invariance in the Mott phase (to all orders in  $t/U$ ), using charge-conjugation symmetry. At intermediate  $U$  the ASL phase occurs for a wide range of  $t'$  which narrows down as  $U$  is increased. Concrete schemes to realize this model have been proposed[20, 28], and experimental methods to probe the semi-metal at low  $U$ [23] and the ASL at large  $U$ [27] exist. This demonstration of the existence of the ASL might help better understand the physics of the pseudo-gap phase of the underdoped high temperature superconductors[8, 9, 29].

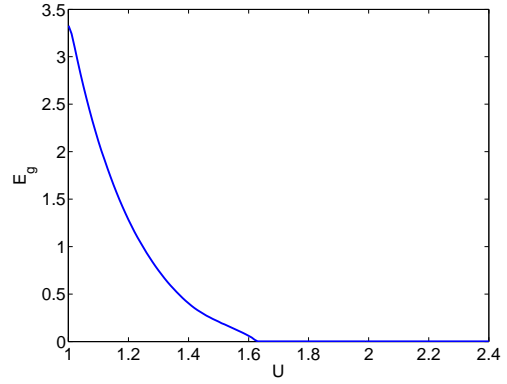


FIG. S4: (color online) Gap of the spinon spectrum as a function of  $U$  for  $t' = 1$

We thank G. Baskaran, André-Marie Tremblay, Mukul Laad for useful discussions and R. Adhikari for feedback on the manuscript. Computational resources were provided by Compute Canada, Calcul Québec and Anna-purna IMSc.

- 
- [1] P. Fazekas and P. Anderson, *Philosophical Magazine* **30**, 423 (1974).
  - [2] P. Anderson, *Science* **235**, 1196 (1987).
  - [3] G. Baskaran and P. W. Anderson, *Phys. Rev. B* **37**, 580 (1988).
  - [4] T. Senthil and M. Fisher, *Physical Review B* **62**, 7850 (2000).
  - [5] X.-G. Wen, *Phys. Rev. B* **65**, 165113 (2002).
  - [6] Y. Shimizu, K. Miyagawa, K. Kanoda, M. Maesato, and G. Saito, *Phys. Rev. Lett.* **91**, 107001 (2003).
  - [7] I. Affleck and J. B. Marston, *Phys. Rev. B* **37**, 3774 (1988).
  - [8] W. Rantner and X.-G. Wen, *Phys. Rev. Lett.* **86**, 3871 (2001).
  - [9] T. Senthil and P. A. Lee, *Phys. Rev. B* **71**, 174515 (2005).
  - [10] A. Kitaev, *Annals of Physics* **321**, 2 (2006).
  - [11] G. Baskaran, S. Mandal, and R. Shankar, *Phys. Rev. Lett.* **98**, 247201 (2007).
  - [9] K. S. Tikhonov, M. V. Feigel'man, and A. Y. Kitaev, *Phys. Rev. Lett.* **106**, 067203 (2011).
  - [8] S. Mandal, S. Bhattacharjee, K. Sengupta, R. Shankar, and G. Baskaran, *Phys. Rev. B* **84**, 155121 (2011).
  - [14] H. Yao, S.-C. Zhang, and S. A. Kivelson, *Phys. Rev. Lett.* **102**, 217202 (2009).
  - [15] M. Hermele, *Phys. Rev. B* **76**, 035125 (2007).
  - [16] Y.-M. Lu and Y. Ran, *Phys. Rev. B* **84**, 024420 (2011).
  - [17] B. K. Clark, D. A. Abanin, and S. L. Sondhi, *Phys. Rev. Lett.* **107**, 087204 (2011).
  - [18] Z. Meng, T. Lang, S. Wessel, F. Assaad, and A. Muramatsu, *Nature* **464**, 847 (2010).
  - [19] Y. O. Sandro Sorella and S. Yunoki, *Arxiv preprint arXiv:1207.1783* (2012).
  - [20] L.-M. Duan, E. Demler, and M. D. Lukin, *Phys. Rev. Lett.* **91**, 090402 (2003).
  - [21] C. Zhang, V. W. Scarola, S. Tewari, and S. Das Sarma,

Proceedings of the National Academy of Sciences **104**, 18415 (2007).

- [22] S. Hassan, S. Goyal, R. Shankar, and D. Sénéchal, Arxiv preprint arXiv:1201.5874 (2012).
- [23] L. Tarruell, D. Greif, T. Uehlinger, J. Gregor, and T. Esslinger, Nature **483**, 302 (2012).
- [1] D. Sénéchal, D. Perez, and M. Pioro-Ladrière, Phys. Rev. Lett. **84**, 522 (2000).
- [4] M. Potthoff, Eur. Phys. J. B **32**, 429 (2003).
- [7] A. Kitaev, Annals of Physics **321**, 2 (2006).
- [27] C. Sanner, E. J. Su, A. Keshet, W. Huang, J. Gillen, R. Gommers, and W. Ketterle, Phys. Rev. Lett. **106**, 010402 (2011).
- [28] W. V. Liu, F. Wilczek, and P. Zoller, Phys. Rev. A **70**, 033603 (2004).
- [29] X.-G. Wen and P. A. Lee, Phys. Rev. Lett. **76**, 503 (1996).

## Supplementary Information

### Cluster Perturbation theory and the VCA

Cluster Perturbation Theory (CPT) is an approximation scheme for the one-electron Green function  $\mathbf{G}(\omega)$  within Hubbard-like models.[1–3] It proceeds by dividing the infinite lattice  $\gamma$  into a super-lattice  $\Gamma$  of identical clusters of  $L$  sites each (Fig.1 of the main text illustrates the cluster used in this work). The lattice Hamiltonian  $H$  is written as  $H = H_c + H_T$ , where  $H_c$  is the cluster Hamiltonian, obtained by severing the hopping terms between different clusters, which are put into  $H_T$ . Let  $\mathbf{T}$  be the matrix of inter-cluster hopping terms and  $\mathbf{G}^c(\omega)$  the exact Green function of the cluster. Because of the periodicity of the super-lattice,  $\mathbf{T}$  can be expressed as a function of the reduced wave-vector  $\tilde{\mathbf{k}}$  and as a matrix in site indices within the cluster:  $T_{ab}(\tilde{\mathbf{k}})$ . Likewise,  $\mathbf{G}^c$  is a matrix in cluster site indices only, since all clusters are identical:  $G_{ab}^c(\omega)$ . Thus, hopping matrices and Green functions in what follows will be  $\tilde{\mathbf{k}}$ -dependent matrices of order  $L$ , the number of sites within each cluster. The fundamental result of CPT for the system's one-electron Green function is

$$\mathbf{G}^{-1}(\tilde{\mathbf{k}}, \omega) = \mathbf{G}^{c-1}(\omega) - \mathbf{T}(\tilde{\mathbf{k}}) \quad (\text{S11})$$

In practice  $\mathbf{G}^c(\omega)$  is calculated numerically by the Lanczos method and the cluster must be small enough for this to be possible. Because the lattice tiling breaks the original translation invariance of the lattice, a prescription is needed to restore the translation invariance of the resulting Green function. The CPT prescription for this periodization is

$$G(\mathbf{k}, \omega) = \frac{1}{L} \sum_{a,b} e^{-i(\mathbf{k}) \cdot (\mathbf{r}_a - \mathbf{r}_b)} G_{ab}(\mathbf{k}, \omega) \quad (\text{S12})$$

where now  $\mathbf{k}$  belongs to the Brillouin zone of the original lattice and the sum is carried over cluster sites. This formula is exact in both the strong ( $t \rightarrow 0$ ) and the weak ( $U \rightarrow 0$ ) coupling limits.

Once the approximate interacting Green function can be calculated, the spectral function  $A(\mathbf{k}, \omega) = -2 \text{Im} G(\mathbf{k}, \omega)$  follows. From there the density of states  $N(\omega)$  can be calculated by numerically integrating  $A(\mathbf{k}, \omega)$  over wave-vectors and the existence of a spectral gap can be assessed. Numerically, the density of states is always evaluated at a complex frequency with a small imaginary part  $\eta$  that broadens the spectral peaks. By applying a few values of  $\eta$  and extrapolating to  $\eta \rightarrow 0$ , one can detect the presence (or not) of a spectral gap at the Fermi level. This allows us to distinguish between a metal and a Mott insulator.

If we know at what wave-vector the gap first opens up, as is the case at  $t' = 0$  (The Dirac points), then we

can estimate the gap more reliably, without the need to extrapolate to  $\eta \rightarrow 0$ , by simply looking up the Lehmann representation of the CPT Green function, which can be calculated when the cluster Green function is computed using the band Lanczos method.

The Variational Cluster Approximation (VCA) is an extension of CPT in which parameters of the cluster Hamiltonian  $H_c$  may be treated variationally, according to Potthoff's Self-Energy Functional Theory (SFT).[4, 5] In particular, it allows the emergence of spontaneously broken symmetries and provides an approximate value for the system's grand potential  $\Omega$ . In the case at hand,

a single variational parameter is used: the strength  $M_c$  of a staggered magnetization field that is added to the cluster Hamiltonian:

$$H_M = M \sum_{\alpha} m_{\alpha} c_{\alpha}^{\dagger} c_{\alpha} \quad (\text{S13})$$

where the symbol  $m_{\alpha}$  is +1 for spin-up orbitals on the A sublattice and spin-down orbitals on the B sublattice, and  $-1$  otherwise.

Technically, VCA proceeds by minimizing the following quantity:

$$\Omega(M_c) = \Omega_c(M_c) - \int \frac{d\omega}{\pi} \frac{d^2 k}{(2\pi)^2} \sum_{\tilde{\mathbf{k}}} \ln \det [\mathbf{1} - \mathbf{T}(\tilde{\mathbf{k}}) \mathbf{G}(\tilde{\mathbf{k}}, i\omega)] \quad (\text{S14})$$

where  $\Omega_c(M_c)$  is the grand potential of the cluster alone (obtained in the exact diagonalization process). The integral over frequencies is carried over the positive imaginary axis. At the optimal value  $M_c^*$ ,  $\Omega(M_c^*)$  is the best estimate of the system's grand potential. At this value of  $M_c$ , the order parameter  $M$  is calculated:

$$M = \int \frac{d^2 \tilde{k}}{(2\pi)^2} \int \frac{d\omega}{2\pi} m_{\alpha} G_{\alpha\alpha}(\tilde{\mathbf{k}}, i\omega) \quad (\text{S15})$$

where  $G_{\alpha\alpha}$  are the diagonal elements of the CPT Green function (S11).

VCA provides estimates of order parameters, much like mean-field theory, but is quite superior to it because the Hamiltonian remains fully interacting (no factorization of the interaction) and spatial correlations are treated exactly within the cluster.

In this work, the VCA was used to find the phase boundary of the antiferromagnetic phase. On the other hand, the transition between the spin liquid and semi-metal phases was found by monitoring the closure of the gap via CPT only.

### Proof of time reversal symmetry in the Mott Phase

In this section we will outline the derivation of the effective spin Hamiltonian and prove that it is time reversal (TR) invariant in the Mott phase.

#### Notation

The Hamiltonian is taken to be:

$$H = \mathcal{H}_0 + \mathcal{H}_K \quad (\text{S16})$$

$$\mathcal{H}_0 = U \sum_i n_{i\uparrow} n_{i\downarrow} \quad (\text{S17})$$

$$\mathcal{H}_K = \sum_{\langle ij \rangle_a} \left\{ c_i^{\dagger} \left( \frac{t + t' \sigma_a}{2} \right) c_j + \text{H.c} \right\} \quad (\text{S18})$$

Let  $P_m$  represent the projector on the Hilbert subspace containing  $m$  doubly occupied sites. Thus  $P_m^2 = P_m$  and  $\sum_{m=0}^{\infty} P_m = 1$ .

We write the Hamiltonian as

$$H = \mathcal{H}_0 + T_0 + T_1 + T_{-1} \quad (\text{S19})$$

$$T_s = \sum_{m=0}^{\infty} P_{s+m} \mathcal{H}_K P_m \quad (\text{S20})$$

$s = -1, 0, 1$ ,  $P_{-1} \equiv 0$ ,  $T_{-s} = T_s^{\dagger}$  and  $T_s$  increases the doubly occupied sites by  $s$ . Thus we have

$$[\mathcal{H}_0, T_s] = sUT_s \quad (\text{S21})$$

The operators that commute with  $\mathcal{H}_0$  are called *block diagonal* (BD) and the others *off block diagonal* (OBD).

### Canonical Perturbation Theory

We follow the approach of Chernyshev *et al.*[6] and block diagonalize the Hamiltonian order by order in  $t/U$ . The  $(k+1)^{th}$  order Hamiltonian is written as

$$\mathcal{H}^{(k+1)} = e^{S^{(k)}} e^{S^{(k-1)}} e^{S^{(k-2)}} \dots H \dots e^{-S^{(k-2)}} e^{-S^{(k-1)}} e^{-S^{(k)}} \quad (\text{S22})$$

$S^{(k)}$  is chosen so as to eliminate the OBD terms of order  $(\frac{t}{U})^k$  that survive in the Hamiltonian after performing the canonical transformation at order  $k-1$ . By construction,  $S^{(k)}$  does not contain terms that preserve the number of doubly occupied sites.

$S^{(k)}$  has to satisfy the equation

$$[S^{(k)}, \mathcal{H}_0] = -\mathcal{H}_{\text{OBD}}^k \quad (\text{S23})$$

where  $\mathcal{H}_{\text{OBD}}^{(k)}$  is the OBD part of  $\mathcal{H}^{(k)}$ . It is easy to show that

$$S^{(k)} = \sum_{i \neq j} \frac{1}{U(i-j)} P_i \mathcal{H}^{(k)} P_j \quad (\text{S24})$$

The effective spin Hamiltonian at half-filling,  $H^{(k)}$ , is obtained by projecting  $\mathcal{H}^{(k)}$  onto the singly occupied subspace.

#### Charge conjugation and Time reversal symmetries

The Hamiltonian (S16) is symmetric under charge conjugation (C) (particle-hole) transformation:

$$U_C c_{i\sigma}^\dagger U_C^\dagger = \eta_i c_{i\sigma} \quad (\text{S25})$$

where  $\eta_i$  is +1 on sublattice A and -1 on sublattice B. The unitary operator  $U_C$  can be explicitly written as

$$U_C = \prod_i e^{i\pi S_i^y} e^{i\pi G_i^y} \quad (\text{S26})$$

where  $S_i^a$  are the spin operators acting on the singly occupied states and  $G_i^a$  are the pseudo-spin operators acting on the empty and doubly occupied states, and defined as

$$G_i^z = \frac{1}{2} (n_{\uparrow i} + n_{\downarrow i} - 1) \quad (\text{S27})$$

$$G_i^+ = c_{\uparrow}^\dagger c_{\downarrow}^\dagger = (G_i^-)^\dagger \quad (\text{S28})$$

Every term in the Hamiltonian,  $\mathcal{H}_0$  and  $T_s$ , is C invariant:

$$U_C H U_C^\dagger = H \quad (\text{S29})$$

$$U_C T_s U_C^\dagger = T_s \quad (\text{S30})$$

It then follows from equations (S24) and (S22) that every term of  $H^k$  is C invariant, for all  $k$ .

The time reversal operator is

$$U_T c_{i\sigma}^\dagger U_T^\dagger = i\sigma_{\sigma\sigma'}^y c_{i\sigma'} \quad (\text{S31})$$

$$U_T = \prod_j e^{i\pi S_j^y} \mathcal{K} \quad (\text{S32})$$

where  $\mathcal{K}$  is the complex conjugation operator. Any state  $|\text{hf}\rangle$  in the singly occupied subspace satisfies the condition  $G_i^a |\text{hf}\rangle = 0$ . It then follows that

$$U_C U_T |\text{hf}\rangle = \mathcal{K} |\text{hf}\rangle \quad (\text{S33})$$

#### Time reversal symmetry of $H^{(k)}$

We show the TR symmetry of  $H^{(k)}$  by explicitly showing the equality of the matrix elements of  $H^{(k)}$  and  $U_T H^{(k)} U_T^\dagger$  in a real basis. Specifically, we can choose the simultaneous eigenstates of  $S_i^z$ ,

$$S_i^z |\{\sigma_i\}\rangle = \frac{1}{2} \sigma_i |\{\sigma_i\}\rangle \quad (\text{S34})$$

We can always choose  $S_i^z$  to be real and hence we have  $\mathcal{K} |\{\sigma_i\}\rangle = |\{\sigma_i\}\rangle$ . It then follows that,

$$\begin{aligned} \langle \{\sigma_i\} | U_T H^{(k)} U_T^\dagger | \{\sigma_i'\} \rangle &= \langle \{\sigma_i\} | U_T^\dagger U_C^\dagger U_C H^{(k)} U_C^\dagger U_T | \{\sigma_i'\} \rangle \\ &= \langle \{\sigma_i\} | \mathcal{K} H^{(k)} \mathcal{K} | \{\sigma_i'\} \rangle = \langle \{\sigma_i\} | H^{(k)} | \{\sigma_i'\} \rangle \end{aligned} \quad (\text{S35})$$

Thus the effective spin Hamiltonian is TR symmetric. This implies that it does not contain any odd-spin terms.

#### Spin-Spin Correlation function

We now outline the computation of the spin-spin correlation function. We write the Hamiltonian as

$$H = \mathcal{H}_0 + \mathcal{H}_p \quad (\text{S36})$$

$$\mathcal{H}_0 = I \sum_{\alpha} S_{\alpha}^{\alpha} S_{\alpha}^{\alpha} \quad (\text{S37})$$

$$\mathcal{H}_p = \sum_{\substack{\langle ij \rangle_\alpha \\ \alpha \neq \beta}} \delta_1 S_i^\beta S_j^\beta + \gamma_1 [S_i^\alpha S_j^\beta + S_j^\alpha S_i^\beta] + \sum_{\langle\langle ij \rangle\rangle_{\alpha\beta}} [\delta_2 \mathbf{S}_i \cdot \mathbf{S}_j + \delta_3 (S_i^\alpha S_j^\alpha + S_i^\beta S_j^\beta) + \gamma_2 S_i^\alpha S_j^\beta] \quad (\text{S38})$$

$$J = \left( \frac{1+t'^2}{U} - \frac{1+t'^4}{U^2} \right); \gamma_1 = -\frac{2t'^2}{U^3}; \gamma_2 = \frac{3t'^2}{U^3} \quad (\text{S39})$$

$$\delta_1 = \frac{t'^4 - 1}{U^3}; \delta_2 = \frac{(1-t'^2)^2}{4U^3}; \delta_3 = \frac{t'^2 - t'^4}{2U^3} \quad (\text{S40})$$

We take the Hamiltonian  $\mathcal{H}_0$  (the Kitaev model) as the unperturbed Hamiltonian and  $\mathcal{H}_p$  as a perturbation. We want to compute the correlation function

$$g(\mathbf{r}, t) = \left\langle T \left( S_{\mathbf{r}l}^\alpha(t) S_{\mathbf{0}m}^\beta(0) \right) \right\rangle \quad (\text{S41})$$

Where  $\mathbf{r} = r_1 \mathbf{e}_1 + r_2 \mathbf{e}_2$ ,  $\mathbf{e}_1$  and  $\mathbf{e}_2$  are basis vectors as shown in Fig.(S5) and  $l, m$  are the sub-lattice indices.

To leading order, this is the spin-spin correlation function of the Kitaev model. The Kitaev model has a 6-spin conserved operator associated with every plaquette,  $W_p$  which can take values  $\pm 1$  and can be interpreted as a  $Z_2$  flux.[7] The ground state is in the flux-free sector ( $W_p = 1 \forall p$ ). The spin operators at site  $\mathbf{r}$  create a pair of flux tubes in two of the plaquettes that the site belongs to. Since the time evolution does not change the flux configuration, the spin-spin correlation (S41) is zero except when  $\mathbf{r}$  and  $\mathbf{0}$  are nearest neighbors.[8]

The second-order perturbation term is

$$g^{(2)} = \frac{(-i)^2}{2} \int d\tau_1 \int d\tau_2 \left\langle T \left( S_{\mathbf{r}l}^\alpha(t) \mathcal{H}_p(\tau_1) \mathcal{H}_p(\tau_2) S_{\mathbf{0}m}^\beta(0) \right) \right\rangle. \quad (\text{S42})$$

The time evolution is governed by  $\mathcal{H}_0$ . This term will be non-zero only if there are terms in  $\mathcal{H}_p$  such that the product of the four operators in (S42) do not change the flux configuration of the ground state.[8] We find that such terms do exist in  $\mathcal{H}_p$ . We concentrate on correlation function  $\langle S_{r_1, r_2, A}^z S_{0, 0, A}^z \rangle$ . The following terms combine with  $S_{r_1, r_2, A}^z$  to produce flux-free configurations when acting on the ground state,

$$\begin{aligned} & \gamma_2 S_{r_1-1, r_2, B}^x S_{r_1-1, r_2+1, B}^y; \quad \gamma_2 S_{r_1+1, r_2-1, A}^x S_{r_1+1, r_2, A}^y; \\ & \gamma_1 S_{r_1, r_2, A}^x S_{r_1-1, r_2+1, B}^y; \quad \gamma_1 S_{r_1, r_2, A}^y S_{r_1-1, r_2, B}^x; \\ & \gamma_1 S_{r_1, r_2, B}^x S_{r_1+1, r_2, A}^y; \quad \gamma_1 S_{r_1, r_2, B}^y S_{r_1+1, r_2-1, A}^x \end{aligned} \quad (\text{S43})$$

These and the terms with  $(r_1, r_2) \rightarrow (0, 0)$  which combine with  $S_{0, 0, A}^z$  give 36 possibly non-zero contributions to  $g^{(2)}$ .

The problem now is to compute the resulting 6-spin correlation functions in the Kitaev model. We do this in the fermionic representation of the spins in an enlarged Hilbert space,[7] in which the Majorana fermion operators  $c_i$  and  $b_i^\alpha$  are defined as follows:

$$\sigma_i^\alpha = ic_i b_i^\alpha, \quad \{c_i, c_j\} = 2\delta_{ij} \quad (\text{S44})$$

$$\{b_i^\alpha, b_j^\beta\} = 2\delta_{\alpha\beta} \delta_{ij}, \quad \{c_i, b_j^\alpha\} = 0 \quad (\text{S45})$$

The physical subspace is defined by the constraint

$$c_i b_i^x b_i^y b_i^z |\psi\rangle_{\text{phys}} = |\psi\rangle_{\text{phys}} \quad (\text{S46})$$

In terms of these Majorana fermions, the leading order Hamiltonian is,

$$\mathcal{H}_0 = J \sum_{\langle ij \rangle_\alpha} ic_i c_j ib_i^\alpha b_j^\alpha \quad (\text{S47})$$

This Hamiltonian describes Majorana fermions ( $c_i$ ), which we refer to as spinons, propagating in the background of static  $Z_2$  gauge fields ( $u_{\langle ij \rangle_\alpha} = ib_i^\alpha b_j^\alpha$ ). The correlation function in equation (S42) thus factorizes into propagators of the  $c_i$  operators. Since the spin operators create two units of flux on adjoining plaquettes, the Majorana fermion propagators are in the background of an even number of fluxes at a few points.

We are interested in the asymptotic form of  $g^{(2)}(\mathbf{r}, t)$  when  $|\mathbf{r}|, t \rightarrow \infty$ . Tikhonov *et. al.* [9] have shown that in this limit, the propagators are the same as those in the flux-free background. Their result can be physically understood by noting that the particles hopping far way from the flux pairs will not pick up any phases from them. Thus we can expect the long wavelength modes to be insensitive to a few localized flux pairs.

To compute the asymptotic form or the propagators, we can derive the continuum theory of the low-energy modes in the flux-free background. The Hamiltonian (S47), when  $ib_i^\alpha b_j^\alpha = 1$ , reduces to nearest-neighbor hopping on a honeycomb lattice just as in graphene.



Graphene has low-energy Dirac quasi-particles about two points,  $\mathbf{K}$  and  $\mathbf{K}'$ , in the Brillouin zone. However, since the  $c$  fermions are Majorana fermions, the excitations exist only over half the Brillouin zone. Thus the low-energy modes constitute a single Dirac quasi-particle. The continuum theory is derived by introducing slowly varying fields  $\psi_l(\mathbf{r})$  such that

$$c_{\mathbf{r}l} = \frac{1}{2} \left( e^{i\mathbf{K}\cdot\mathbf{r}} \psi_l(\mathbf{r}) + e^{-i\mathbf{K}\cdot\mathbf{r}} \psi_l^\dagger(\mathbf{r}) \right) \quad (\text{S48})$$

Substituting equation (S48) in equation (S47) it can be seen that the low energy continuum theory is that of a

single Dirac fermion. The propagator is defined as

$$G_{lm}(\mathbf{r}, t) = \langle T (\psi_l(\mathbf{r}, t) \psi_m^\dagger(0, 0)) \rangle \quad (\text{S49})$$

It can be computed to be

$$G_{lm} = (\boldsymbol{\tau} \cdot \mathbf{r} - Jt\mathbb{I})_{lm} \frac{1}{4\pi} \frac{1}{(\mathbf{r}^2 - J^2 t^2)^{\frac{3}{2}}} \quad (\text{S50})$$

where  $\boldsymbol{\tau} = (\tau_x, \tau_y)$  are the Pauli matrices. We can then compute the correlation function in equation (S42) to obtain the following expression:

$$\begin{aligned} \langle S_{\mathbf{r}l}^z(t) S_{0l}^z(0) \rangle = & (-0.56 \cos(2\mathbf{K} \cdot \mathbf{r}) \gamma_1^2 + 1.13 \gamma_1 \gamma_2 + 1.69 \gamma_2^2 \epsilon) \det G + (0.56 \gamma_1^2 - 0.28 \gamma_1 \gamma_2 + 0.84 \gamma_1 \gamma_2 \epsilon) \text{Tr}(G \tau_x G) \\ & + (0.28 \gamma_1^2 + 0.07 \gamma_2^2 + 0.84 \gamma_1 \gamma_2 \epsilon + 0.63 \gamma_2^2 \epsilon^2 - 0.28 \gamma_1 \gamma_2 - 0.42 \gamma_2^2 \epsilon) (\text{Tr} G)^2 + 0.28 \gamma_1^2 \text{Tr}(\tau_x G \tau_x G) \end{aligned} \quad (\text{S51})$$

where  $l$  represents the sublattice index (A or B),  $\alpha$  represents the three types of bonds  $x, y, z$  and  $\epsilon$  is the energy density of the Kitaev model. We can obtain the  $\langle S_{\mathbf{r}l}^x(t) S_{0l}^x(0) \rangle$  and  $\langle S_{\mathbf{r}l}^y(t) S_{0l}^y(0) \rangle$  from the above correlation function by using the following property: a  $2\pi/3$  rotation about a sublattice  $A$  point takes  $x$  link to  $y$  link,  $y$  link to  $z$  and  $z$  link to  $x$ , in a cycle. The direction is reversed for sublattice  $B$ . Thus we can see that the (S51) goes as  $r^{-4}$  which shows that we have an algebraic spin liquid (ASL) for large  $U$ .

### Mean Field Theory of the effective spin model

The effective spin Hamiltonian is given in equation (S36). To investigate the instability of the ASL to CSL, we perform a mean-field treatment of the above Hamiltonian in the fermionic representation (S44). The decoupling of the spinon and gauge field sectors is represented by

$$\sigma_i^\alpha \sigma_j^\beta = -i c_i c_j i b_i^\alpha b_j^\beta \quad (\text{S52})$$

$$\approx -i c_i c_j B_{ij}^{\alpha\beta} - i c_{ij} b_i^\alpha b_j^\beta + C_{ij} B_{ij}^{\alpha\beta} \quad (\text{S53})$$

The self-consistency equations are

$$B_{ij}^{\alpha\beta} \equiv \langle i b_i^\alpha b_j^\beta \rangle; \quad C_{ij} \equiv \langle i c_i c_j \rangle \quad (\text{S54})$$

We assume that the ground state is translationally invariant, isotropic and denote

$$C_{i,i+\mathbf{a}_\alpha} = \epsilon; \quad B_{i,i+\mathbf{a}_\alpha}^{\alpha\alpha} = \eta; \quad C_{i,i\pm\mathbf{e}_i,l} = \mu_l; \quad (\text{S55})$$

$$B_{i,i+\mathbf{a}_\alpha}^{\alpha\beta} = B_\alpha^{\alpha\beta}; \quad B_{i,i\pm\mathbf{e}_i,l}^{\alpha\beta} = b_l; \quad \alpha \neq \beta \quad (\text{S56})$$

where  $\mathbf{a}_\alpha$  represents the nearest neighbor vector on the  $\alpha^{\text{th}}$  link.  $\alpha, \beta$  represent the links  $(x, y, z)$ ,  $l$  indicates the sublattice index (A or B) and  $\mathbf{e}_i$  represents the basis vectors of the underlying Bravais lattice (see Fig: S5).

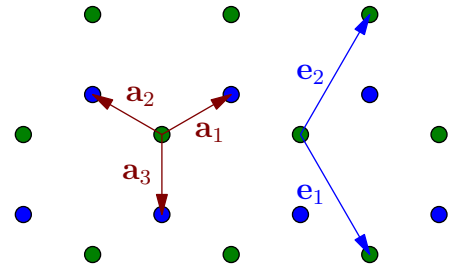


FIG. S5: Basis vector used. Green (Blue) represents sublattice A (B).

The mean field Hamiltonian at  $t' = 1$  is,

$$H_{MF} = H_{MF}^b + H_{MF}^c \quad (S57)$$

$$H_{MF}^b = \frac{1}{4} \sum_{\mathbf{k} \in \text{HBZ}} \left( (b_{\mathbf{k}1}^\alpha)^\dagger \ (b_{\mathbf{k}2}^\alpha)^\dagger \right) \begin{pmatrix} iV_{\alpha\beta,1}(\mathbf{k}) & iU_{\alpha\beta}(\mathbf{k}) \\ -iU_{\alpha\beta}^*(\mathbf{k}) & iV_{\alpha\beta,2}(\mathbf{k}) \end{pmatrix} \begin{pmatrix} b_{\mathbf{k}1}^\beta \\ b_{\mathbf{k}2}^\beta \end{pmatrix} \quad (S58)$$

$$U(\mathbf{k}) = \epsilon \begin{pmatrix} J e^{-ik_1} & \gamma_1(e^{-ik_1} + e^{ik_2}) & \gamma_1(e^{-ik_1} + 1) \\ \gamma_1(e^{-ik_1} + e^{ik_2}) & J e^{ik_2} & \gamma_1(e^{ik_2} + 1) \\ \gamma_1(e^{-ik_1} + 1) & \gamma_1(e^{ik_2} + 1) & J \end{pmatrix} \quad (S59)$$

$$V_{\alpha\beta,1} = \mu_1 \gamma_2 \begin{pmatrix} 0 & e^{ik_3} & -e^{-ik_1} \\ -e^{-ik_3} & 0 & e^{ik_2} \\ e^{ik_1} & -e^{-ik_2} & 0 \end{pmatrix} \quad (S60)$$

$$V_{\alpha\beta,2} = \mu_2 \gamma_2 \begin{pmatrix} 0 & -e^{-ik_3} & -e^{-ik_1} \\ e^{ik_3} & 0 & -e^{-ik_2} \\ e^{ik_1} & e^{ik_2} & 0 \end{pmatrix} \quad (S61)$$

$$H_{MF}^c = \frac{1}{4} \sum_{\mathbf{k} \in \text{HBZ}} \left( c_{\mathbf{k}1}^\dagger \ c_{\mathbf{k}2}^\dagger \right) \begin{pmatrix} i v_1(\mathbf{k}) & i u(\mathbf{k}) \\ -i u^*(\mathbf{k}) & i v_2(\mathbf{k}) \end{pmatrix} \begin{pmatrix} c_{\mathbf{k}1} \\ c_{\mathbf{k}2} \end{pmatrix} \quad (S62)$$

$$u(\mathbf{k}) = \sum_{\alpha} e^{-i\mathbf{k} \cdot \mathbf{e}_{\alpha}} \left( J\eta + \gamma_1 \sum_{\beta \neq \alpha} B_{\alpha}^{\beta} \right) \quad (S63)$$

$$v_1(\mathbf{k}) = 2ib_1\gamma_2 \sum_{\alpha} \sin(\mathbf{k} \cdot \mathbf{e}_{\alpha}) \quad (S64)$$

$$v_2(\mathbf{k}) = -2ib_2\gamma_2 \sum_{\alpha} \sin(\mathbf{k} \cdot \mathbf{e}_{\alpha}) \quad (S65)$$

where  $k_i = \mathbf{k} \cdot \mathbf{e}_i$

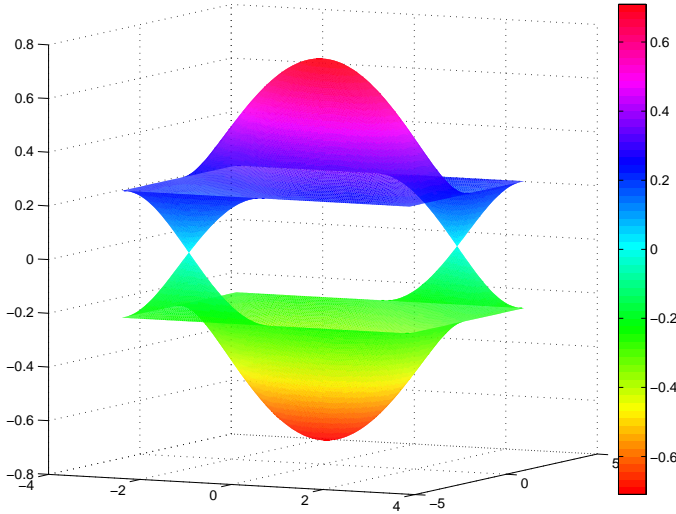


FIG. S6: Spinon dispersion relation at  $U = 2$ .

The nearest-neighbor term in Hamiltonian (S36) results in closing the gap in the spinon sector at the Dirac points (see Fig: S6), whereas the next-nearest term collapses the gap at  $(0,0)$  and  $(\pi,\pi)$ . For large values of  $U$  the nearest-neighbor term dominates; for smaller values of  $U$ , on the other hand, the next-nearest neighbor

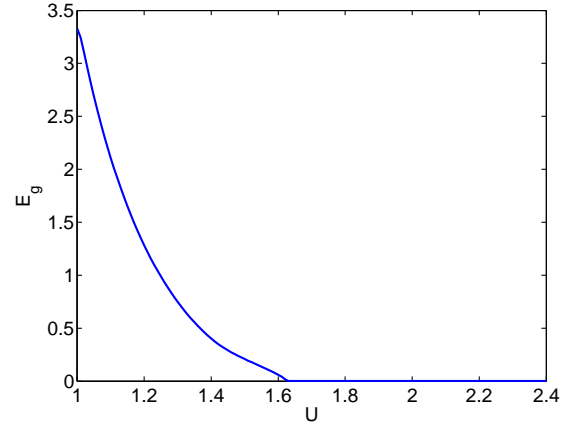


FIG. S7: Spinon gap,  $E_g$  as a function of  $U$ .

term comes into play and the Dirac points shift to  $(0,0)$  and  $(\pi,\pi)$ . Numerically we find that the spinon sector is gap-less for  $U \geq 1.6$  (see Fig:S7). We have checked that this remains true for  $1 < t' < 0.5$ . VCA indicates a Mott transition at  $U = 2.4$ . This shows the absence of the CSL phase in the presence of higher order perturbative terms and indicates the ASL phase continues till the Mott transition.

- 
- [1] D. Sénéchal, D. Perez, and M. Pioro-Ladrière, Phys. Rev. Lett. **84**, 522 (2000).
  - [2] D. Sénéchal, D. Perez, and D. Plouffe, Phys. Rev. B **66**, 075129 (2002).
  - [3] D. Sénéchal, in *Theoretical methods for Strongly Correlated Systems*, edited by A. Avella and F. Mancini (Springer, 2012), vol. 171 of *Springer Series in Solid-State Sciences*, chap. 8, pp. 237–269.
  - [4] M. Potthoff, Eur. Phys. J. B **32**, 429 (2003).
  - [5] M. Potthoff, in *Theoretical methods for Strongly Correlated Systems*, edited by A. Avella and F. Mancini (Springer, 2012), vol. 171 of *Springer Series in Solid-State Sciences*, chap. 9.
  - [6] A. L. Chernyshev, D. Galanakis, P. Phillips, A. V. Rozhkov, and A.-M. S. Tremblay, Phys. Rev. B **70**, 235111 (2004).
  - [7] A. Kitaev, Annals of Physics **321**, 2 (2006).
  - [8] S. Mandal, S. Bhattacharjee, K. Sengupta, R. Shankar, and G. Baskaran, Phys. Rev. B **84**, 155121 (2011).
  - [9] K. S. Tikhonov, M. V. Feigel'man, and A. Y. Kitaev, Phys. Rev. Lett. **106**, 067203 (2011).